

Comparison of Torque Performances on Different Core Material for Switched Reluctance Actuator without Permanent Magnet

I, Yusri¹, M., M. Ghazaly¹, R., Ranom¹, M. F., Rahmat², I. W., Jamaludin¹

¹Center for Robotics and Industrial Automation (CeRIA), Faculty of Electrical Engineering, Universiti Teknikal Malaysia Melaka, Hang Tuah Jaya, 76100 Durian Tunggal, Melaka, Malaysia.

²Faculty of Electrical Engineering, Universiti Teknologi Malaysia, 81310 UTM Johor Bahru, Johor, Malaysia.

mariam@utem.edu.my

Abstract— This paper presents the comparison of torque profiles of the Switched Reluctance Actuator (SRA) without permanent magnet (PM) using two types of materials which are Low Carbon steel, Grade 1008 and Medium Carbon steel, Grade S45C. Each of the Low Carbon steel and Medium Carbon steel is distinguished by the percentage of carbon contents which is 0.1% and 0.43%, respectively. The designed SRA of both materials was according to the size of NEMA 17 standard stepper motor for small machine applications and simulated through FEM analysis. The maximum generated torque achieved by the SRA with the Low Carbon steel is 122.540mNm and with Medium Carbon steel is 54.107mNm, respectively at 2A input current. It shows that the carbon content influences the magnetic properties of the materials as the generated torque decreases approximately 50% when the carbon content is four (4) times higher. As a conclusion, the Medium Carbon steel, Grade S45C depict better working range as it capable of generating high torque at a small overlapping angle compared to Low Carbon steel, Grade 1008.

Index Terms— Carbon steel; FEM analysis; SRA; Torque.

I. INTRODUCTION

There are many types of rotary actuators available in the market today that are built for specific applications such as in manufacturing robotic. A typical actuator contains mechanical components like rotor, shaft, stator, and windings. However, as the demand for high torque application increases, most of the actuator manufacturing industries adopted the rare-earth materials in the design. Thus, the cost for manufacturing increases along and caused a lot of unwanted waste products as these materials are non-environmental friendly [1]. Due to this reason, research development of free rare-earth material actuator types is aggressively conducted to replace the present's actuator [2], [3]. Switched Reluctance Actuator (SRA) is one of the suitable candidates to fulfill these requirements. It is an incremental-drive typed actuator which is sub-grouped under the stepper motor. SRA has several advantages such as simple structure, low cost, compact and maintenance free. It is commonly used in precision application such as Pick-and-Place (P&P) machine. However, its faces with some drawbacks such as low efficiency, high noise and torque ripple and also low output torque.

Most of the previous researchers conducted in the development of the SRA, uses high-quality ferromagnetic

materials such as silicone steel [4], [5]. Its high permeability and conductivity properties are undeniable due to the high silicone contents which lead to better performances and comparable with the permanent magnet machine. However, the problems of materials availability in Malaysia cannot be avoided. The production of silicone steel material is limited, and most of them were imported from other countries. Thus, substitution of these materials is required such that it is readily available and frequently used materials in Malaysia such as carbon steel.

Carbon steel has been used in many applications due to its mechanical strength capabilities as shown in Table 1. It can be found in most construction industry for underground piping systems, built beams and platforms. On top of that, due to its toughness and strength properties, it already is being used for torsion bars, crankshafts, bolts, and axles as well. Thus, the built actuator using this material can be suited for the harsh environment applications such as in heating furnaces or even in motoring systems in the car. Apart from the strength, it also a can be categorized as ferromagnetic materials since it is composed of silicone material as shown in Table 2.

Table 1
Mechanical Properties and Machinability of Steel bar

| Steel Grade | Tensile Strength, Mpa | Yield Strength, Mpa | Elongation, % | Maximum temperature, °C |
|-------------|-----------------------|---------------------|---------------|-------------------------|
| 1008 | 303 | 170 | 30 | 1232 |
| S45C | 630 | 530 | 12 | 779 |

Table 2
Chemical Composition of Steel

| Steel grade | Chemical Composition Limit, % | | | | |
|-------------|-------------------------------|---------------|---------------|------------|--------------|
| | Carbon, C | Manganese, Mn | Phosphorus, P | Sulphur, S | Silicone, Si |
| 1008 | 0.10 | 0.30 | 0.04 | 0.05 | 0.10 |
| S45C | 0.43 | 0.6 | 0.04 | 0.05 | 0.10 |

Therefore, this paper will discuss the generated torque performances based on the Finite Element Analysis (FEM) for different carbon steel materials. ANSYS Maxwell 3D software was chosen for the analysis in this research to identify the generated static torque. Similar optimized design

done in the previous research is adopted using Low Carbon steel, Grade 1008 and Medium Carbon steel, Grade S45C [6, 7]. In section 2, this paper discusses the properties of the chosen materials and design of the SRA that have been adopted throughout the research. The effect of carbon content on the composition of the material is discussed further for comparison purposes. In Section 3, the generated torque performance is discussed by presents the torque profile of the SRA. The influence of magnetic flux linkage towards the generated torque is also has been analyzed. Finally, Section 4 concludes the finding of the research based on the comparisons of the two materials.

II. METHODOLOGY

The SRA is operated based on the electromagnetism principle which adopts switching reluctance between the phases. The pathway with a low reluctance through the air-gap allows the concentration of magnetic flux to form in the core. As the poles energized continuously, the accumulated magnetic flux increases. The nearest rotor’s pole will build the flux linkage between the stator and rotor poles and hence generates the torque. Since the SRA experienced with high torque ripple, its positioning is the crucial part to be predetermined in this research. Thus, in order to determine the basic characteristic of the SRA, the rotor will be assigned to several positions, and its generated torque is analyzed.

The conventional SRA design normally consists of three materials which are the stator and rotor core, coil winding and permanent magnet (PM). In this research, only two materials which are ferromagnetic material for stator and rotor core and the copper wire for coil winding are implemented for the SRA design which is highly cost effective. Figure 1 and Table 3 show the geometrical design of the SRA for stator-to-rotor poles ratio, S:R=6:4 configurations and its parameters, respectively. The label of SRA is shown in Table 4. The design was modified from the conventional hybrid stepper motor, NEMA 17 which is commonly used in small machine applications such as a 3D printer, pick and place machine, medical instruments and prototyping machines. In this paper, the presented result of generated torque utilized the same design and configuration of the SRA for both types of materials. Both materials underwent simulations with excitation current range from 0A to 2A with an interval of 0.5A. The rotor was rotated such that it positioned from unaligned position (0°) to unaligned position (80°) for single phase’s full working range. The generated torque was compiled at each interval of 2°.

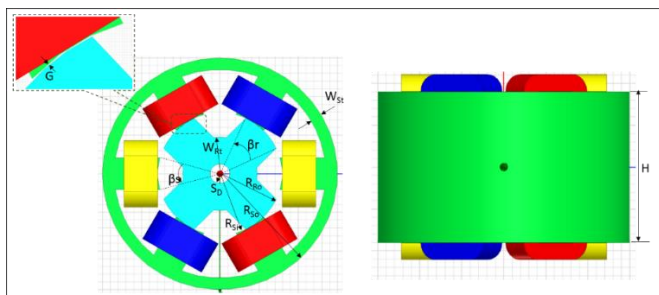


Figure 1: SRA Geometrical Construction

Table 3
SRA Parameters

| Parameters | Value |
|---------------------------------|----------|
| Stator outer diameter, R_{So} | 60 mm |
| Stator inner diameter, R_{Si} | 31.8 mm |
| Rotor outer diameter, R_{Ro} | 31.6 mm |
| Air gap thickness, G | 0.2 mm |
| Winding number | 60 Turns |
| Stator and rotor height, H | 36 mm |
| Stator arc angle, β_s | 29° |
| Rotor arc angle, β_r | 40° |
| Rotor thickness, W_{Rt} | 5 mm |
| Stator thickness, W_{St} | 3 mm |
| Shaft hole diameter, S_D | 5 mm |

Table 4
SRA Label

| Part | Label |
|-----------------|--------|
| Stator | Green |
| Rotor | Cyan |
| Winding Phase A | Red |
| Winding Phase B | Yellow |
| Winding Phase C | Blue |

Two types of materials were chosen in this research for analysis which is Low Carbon steel Grade 1008 and Medium Carbon steel Grade S45C. Both materials are distinguished by the percentage of carbon contents. However, these materials have approximately the same amount of silicone element which is 0.1%. Hence, the conductivity characteristic is dominantly determined by the carbon contents. The relationship of flux density, B, and magnetic field strength, H can be illustrated using a B-H curve, as shown in Figure 2. It can be depicted that both materials have approximately similar maximum saturation level which is 1.9T, respectively. Nonetheless, Low Carbon steel Grade 1008 exhibits higher flux density at low magnetic field compared to the Medium Carbon steel Grade S45C. In comparison with the high-performance ferromagnetic material namely Silicone steel, type 10JNEX900, it has lower saturated magnetic flux density which is at 1.8T. But due to the advantages of low iron loss and low hysteresis own by the silicone steel, it remains as the best ferromagnetic materials for actuators manufacturing.

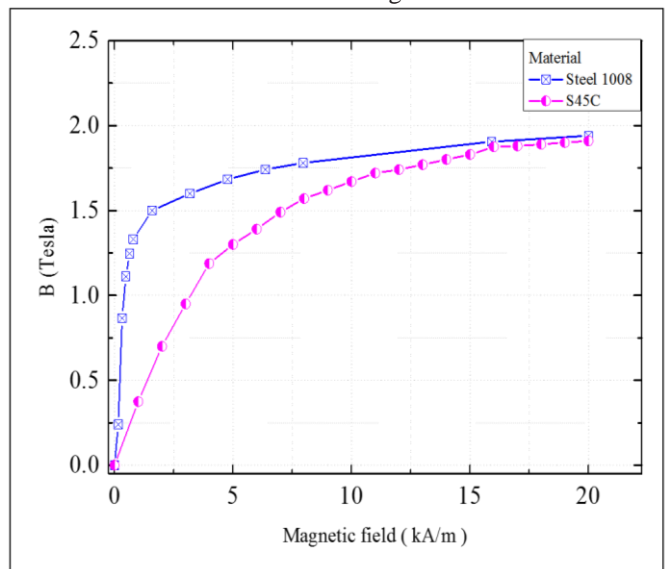


Figure 2: B-H curve of material Low Carbon steel (1008) and Medium Carbon steel (S45C)

III. PERFORMANCE COMPARISON

In this section, the result for both materials are presented and further compared to quantify the variations of magnetic flux, which contribute to the generated torque. The effect of carbon content is analyzed as well.

A. Torque characteristic

Figure 3 (a) and (b) show the results of generated torque profile for Low Carbon steel, grade 1008 and Medium Carbon steel, grade S45C material respectively. The results indicate the tendency of rotation based on the polarity of the generated torque value. It shows that the first half position which is from 0° to 40°; have the tendency of the rotor to rotate in an anti-clockwise direction. Meanwhile, the other half indicates the reverse direction. The pattern for both materials is almost similar. The SRA is capable of generating the highest torque when the maximum excitation current of 2A is applied.

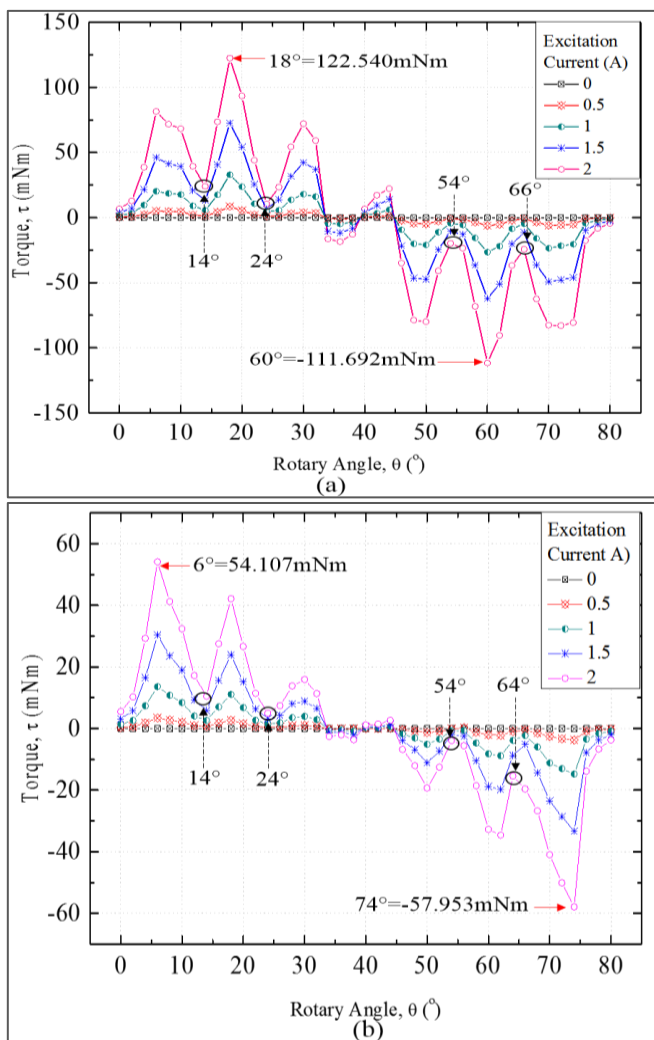


Figure 3: Torque characteristic of (a) Low Carbon steel, Grade 1008 and (b) Medium Carbon steel, Grade S45C

Based on the result, the generated torque for Low Carbon steel is higher compared to the Medium Carbon steel for all excitation current values. As referred to the maximum generated torque, the Low Carbon steel generates torque approximately 50% higher with 122.540mNm compared to the Medium Carbon steel which generates only 54.107mNm. This agrees with the composition of the element for the

materials which the carbon content significantly influences the conductivity of magnetism in the core. The presence of carbon elements established the high reluctance pathways which against the accumulated magnetic flux for full magnetization. Since the simulation SRA was not applied the maximum magnitude of the excitation current, the flux density also built lower as referred to B-H curve shown in Figure 2.

Another observation can be made from the results was the positioning of the rotor pole at the maximum generated torque. It is shown that the generated torque was maximized at position 18° and 6° for Low and Medium Carbon steel respectively. The position was reflected the overlapping angle between the stator and rotor pole which at position 18°, it is overlapped with 13°. Meanwhile, it only overlapped with 1° for position 6°. In can be deduced that, the Low Carbon steel require larger overlapping angle to generate the highest torque compare to the Medium Carbon steel. In practical operations, the Medium Carbon steel can operate better with larger working range since it capable of producing the highest torque with the slightly overlapping angle.

B. Magnetic Flux Linkage

Figure 4 (a) and (b) show the magnetic flux linkage form at Phase A, B, and C with the excitation current of 2A for Low and Medium Carbon steel respectively. Since Phase A was the energized pole, most of the magnetic flux accumulated between its stator pole to the nearest rotor pole. The ideal operation is when the magnetic flux is solely concentrated at the energized pole which is impossible due to the presence of adjacent pole. It can be seen that the magnetic flux tended to form a linkage at another pole. Even though it produces a small magnitude, but the effect is significantly seen as the generated torque was started to decline from position 8° to 14° for both materials. At this moment, Phase B was influenced the most because of low reluctance at the linkage formed between the stator and rotor poles. The concentration of accumulated magnetic flux is reduced as it diffused to the adjacent phase during excitation.

Referring to the position 14° at which the lowest torque is generated as shown in Figure 5 (a); Phase B has higher overlapping angle compared to the Phase A and hence it capable of providing low reluctance pathway for the magnetic flux. Due to the slightly unaligned positioning at Phase B, it tends to rotate the rotor such that it against the targeted direction which is toward clockwise rotation. As a result, the generated torque is reduced as it had to oppose the torque form at the other phases. Meanwhile, the generated torque also produces the lowest when the rotor is at position 24° as shown in Figure 5 (b). At this state, the overlapping angle at Phase A and Phase B is approximately the same such that both phases provide the similar reluctance pathway. It can be seen that the magnetic flux is distributed away from the Phase A and towards the Phase B. Hence, the concentration at the energized pole is reduced and generated torque is dropped.

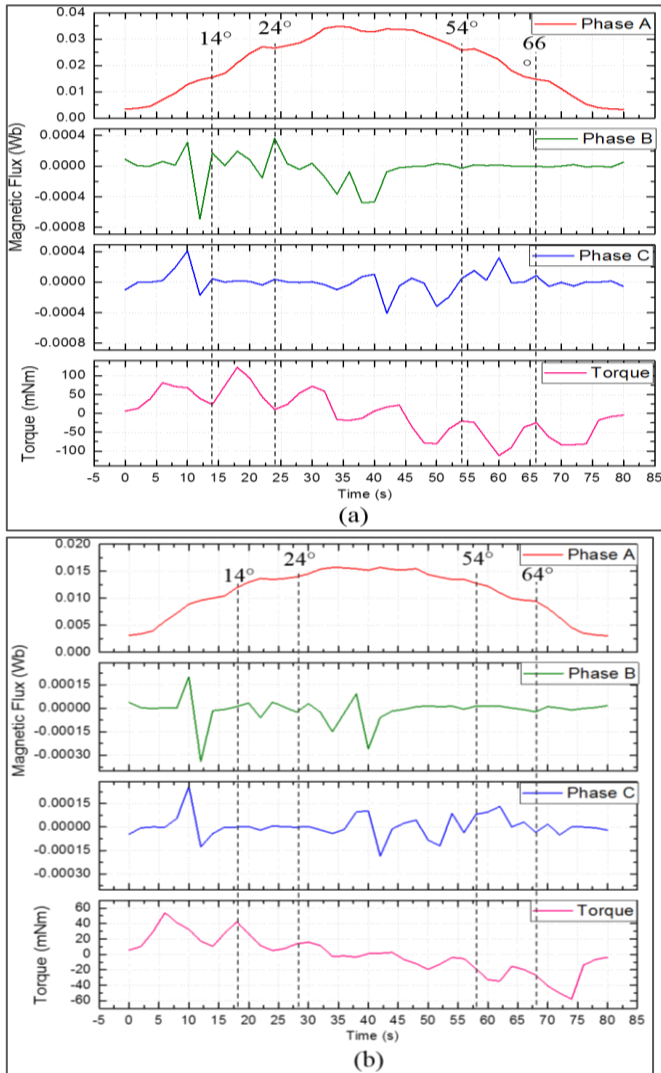


Figure 4: Magnetic flux linkage form at Phase A, B and C for (a) Low Carbon steel, Grade 1008 and (b) Medium Carbon steel, Grade S45C

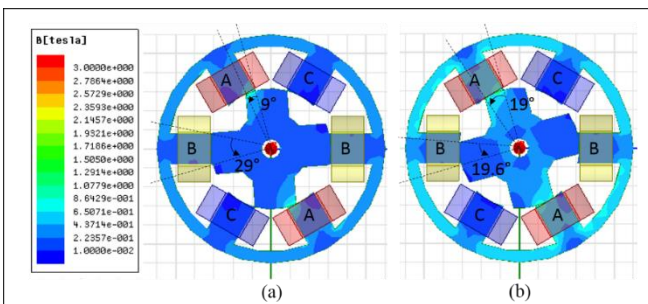


Figure 5: Overlapping angle and magnetic flux distribution of Low Carbon steel, Grade 1008 SRA for the position (a) 14° and (b) 24°

IV. CONCLUSION

In summary, this paper focuses on the comparison of generated torque for two types of material which are Low Carbon steel, Grade 1008 and Medium Carbon steel; Grade

S45C applied to the SRA design without PMs. The torque profiles of each material are presented and compared to determine the torque characteristics and the effects of varying rotor position. The result of flux linkage forms at all phases was collected to observe the characteristic of magnetic flux distribution. Through the FEM analysis, it shows that the Low Carbon steel, Grade 1008 performs better with higher generated torque at all excitation current compared to the Medium Carbon steel, Grade S45C. As a comparison, the carbon content in Medium Carbon steel, Grade S45C is approximately four (4) times higher, and the generated torque is reduced about 50% due to the non-magnetism properties of the carbon. However, Medium Carbon steel, Grade S45C provided better working range especially at the unaligned position, and it had strength capability which made it suitable for the harsh environment.

ACKNOWLEDGMENT

Authors are grateful to Universiti Teknikal Malaysia Melaka (UTeM) and UTeM Zamalah Scheme for supporting the research. This research and its publication are supported by Fundamental Research Grant Scheme (FRGS) no.FRGS/1/2016/TK04/FKE-CERIA/F00305, Motion Control Research Laboratory (MCon Lab), Center for Robotics and Industrial Automation (CeRIA) and Center for Research and Innovation Management (CRIM).

REFERENCES

- [1] A. Saguchi, K. Asabe, T. Fukuda, W. Takahashi, and R. O. Suzuki, "Recycling of rare earth magnet scraps : Carbon and oxygen removal from Nd magnet scraps," vol. 412, pp. 1377–1381, 2006.
- [2] A. Chiba, K. Kiyota, N. Hoshi, M. Takemoto, and S. Ogasawara, "Development of a rare-earth-free SR motor with high torque density for hybrid vehicles," *IEEE Trans. Energy Convers.*, vol. 30, no. 1, pp. 175–182, 2015.
- [3] A. Chiba, M. Takeno, S. S. Member, Y. Takano, N. Hoshi, M. Takemoto, S. Ogasawara, and T. Imakawa, "Torque Density and Efficiency Improvements of a Switched Reluctance Motor Without Rare-Earth Material for Hybrid Vehicles," *IEEE Trans. Ind. Appl.*, vol. 47, no. 3, pp. 1240–1246, 2011.
- [4] H. Hayashi, K. Nakamura, A. Chiba, T. Fukao, K. Tungpimolrut, and D. G. Dorrell, "Efficiency improvements of switched reluctance motors with high-quality iron steel and enhanced conductor slot fill," *IEEE Trans. Energy Convers.*, vol. 24, no. 4, pp. 819–825, 2009.
- [5] Y. Nakazawa, K. Ohyama, K. Nouzuka, H. Fujii, H. Uehara, and Y. Hyakutake, "Design Method for Improving Motor Efficiency of Switched Reluctance Motor," *IEEJ Trans. Ind. Appl.*, vol. 134, no. 7, pp. 656–666, 2014.
- [6] I. Yusri, M. M. Ghazaly, E. A. Alandoli, M. F. Rahmat, Z. Abdullah, M. A. M. Ali, and R. Ranom, "Optimization of the Force Characteristic of Rotary Motion Type of Electromagnetic Actuator Based on Finite Element Analysis," *Proc. Mech. Eng. Res. Day 2016*, pp. 1–2, 2016.
- [7] I. Yusri, M. M. Ghazaly, M. F. Rahmat, S. H. Chong, R. Ranom, Z. Abdullah, S. P. Tee, and C. K. Yeo, "Effects of Varying Arc Angles and Poles Numbers on Force Characteristics of Switched Reluctance (SR) Actuator," *Int. J. Mech. Mechatronics Eng. IJMME-IJENS*, vol. 16, no. 5, pp. 41–47, 2016.